

and in the absence of salt using only two synthetic surfactants. The microstructure of these complex aggregates is sketched in Fig. 4. Self-assembly of icosahedra, owing to defect-free repetition of strong interactions, is one of the fascinating consequences of the quasi-equivalence principle<sup>25</sup>: highly symmetric structures can be formed with high efficiency by association of identical subunits in the absence of templates. The self-assembled two-dimensional nearly crystalline shell is similar in shape to the structure initially proposed for viruses by Watson and Crick<sup>26</sup>. In catanionic icosahedra, subunits are combinations of catanionic pairs. Although in viruses the number of subunits is smaller, the type of aggregates described here should obey a similar topology control mechanism: a locally hexagonal lattice folds into 20 equivalent triangles. The association of anionic and cationic surfactants produces particles similar in shape but larger than viruses. □

Received 14 February; accepted 27 March 2001.

1. Thompson, D. W. *On Growth and Form* (Cambridge Univ. Pres, Cambridge, 1961).
2. Kimoto, K. & Nishida, I. The crystal habits of small particles of aluminium and silver prepared by evaporation in clean atmosphere of argon. *J. Appl. Phys.* **16**, 941–948 (1966).
3. Hubert, H. H. *et al.* Icosahedral packing of B<sub>12</sub> icosahedra in boron suboxide. *Nature* **391**, 376–378 (1998).
4. Sackmann, E. & Lipowsky, R. *Handbook of Biological Physics* Vol. 1B (ed. Hoff, A. J.) (North-Holland, Amsterdam, 1995).
5. Kaler, E. W., Murthy, A. K., Rodriguez, B. E. & Zasadzinski, J. A. N. Spontaneous vesicle formation in aqueous mixtures of single-tailed surfactants. *Science* **245**, 1371–1374 (1989).
6. Dubois, M. & Zemb, T. Swelling limits for bilayer microstructures: the implosion of lamellar structure versus disordered lamellae. *Curr. Opin. Colloid Interf. Sci.* **5**, 27–37 (1997).
7. Wals, J. *et al.* Tricord protease exists as an icosahedral supermolecule *in vivo*. *Molecul. Cell.* **1**, 59–65 (1997).
8. Klug, A., Franklin, R. E. & Humphrey-Owen, S. P. F. The crystal structure of Tipula iridescent virus as determined by Bragg reflection of visible light. *Biochem. Biophys. Acta* **32**, 203–219 (1959).
9. Dubois, M., Gulik-Krzywicki, Th., Demé, B. & Zemb, T. Rigid organic nanodiscs of controlled size: A catanionic formulation. *C. R. Acad. Sci. Paris II C* **1(9)**, 567–575 (1998).
10. Scamehorn, J. F. & Hartwell, J. H. in *Surfactant Science Series* (eds Scamehorn, J. F. & Harwell, J. H.) Vol. 33, Ch. 10 (Marcel Dekker Inc., New York, 1989).
11. Graciaa, A., Ghoulam, M. B., Marion, G. & Lachaise, J. Critical concentrations and compositions of mixed micelles of sodium dodecylbenzenesulfonate, tetradecyltrimethylammonium bromide and polyethylenephenols. *J. Phys. Chem.* **93**, 4167–4173 (1989).
12. Schnur, J. Lipid tubules: a paradigm for molecularly engineered structures. *Science* **262**, 1669–1675 (1993).
13. Thomas, B. N., Safinya, C. R., Plano, R. J. & Clark, N. A. Lipid tubules self-assembly: length dependence on cooling rate through a first-order phase transition. *Science* **227**, 1635–1638 (1995).
14. Parente, R. A., Höchli, M. & Lentz, B. R. Morphology and phase behavior of two types of unilamellar vesicles prepared from synthetic phosphatidylcholines studies by freeze-fracture electron microscopy and calorimetry. *Biochim. Biophys. Acta* **812**, 493–502 (1985).
15. Regev, O., Marques, E. F. & Khan, A. Polymer-induced structural effects on catanionic vesicles: formation of faceted vesicles, disks, and cross-links. *Langmuir* **15**, 642–645 (1999).
16. Zemb, T., Dubois, M., Demé, B., Gulik-Krzywicki, T. Self-assembly of flat nanodiscs in salt-free catanionic surfactant solutions. *Science* **283**, 816–820 (1999).
17. Hyde, S. T. Topological transformations mediated by bilayer punctures: from sponge phases to bicontinuous monolayers and reversed sponges. *Colloids Surf. A* **129–130**, 207–225 (1997).
18. Fogden, A., Daicic, J. & Kidane, A. Undulating charges in fluid membranes and their bending constants. *J. Phys. (Paris)* **II 7**, 229–248 (1997).
19. Fogden, A. & Daicic, J. & Kidane, A. Bending rigidity of ionic surfactant interfaces with variable charge density: the salt-free case. *Colloids Surf. A* **129–130**, 157–165 (1997).
20. Nelson, D. R. & Spaepen, F. Polytetrahedral order in condensed matter. *Solid State Phys.* **42**, 1–90 (1989).
21. Dubois, M., Belloni, L., Zemb, T., Demé, B. & Gulik-Krzywicki, T. Formation of rigid nanodiscs: Edge formation and molecular separation. *Prog. Colloid Polym. Sci.* **115**, 238–242 (2000).
22. Radtchenko, I. L. *et al.* Assembly of alternated multivalent ion/polyelectrolyte layers on colloidal particles. Stability of the multilayers and encapsulation of macromolecules into polyelectrolyte capsules. *J. Colloid Interf. Sci.* **230**, 272–280 (2000).
23. Donath, E., Sukhorukov, G. B., Caruso, F., Davis, S. A. & Möhwald, H. Novel hollow polymer shells by colloid-templated assembly of polyelectrolytes. *Angew. Chem. Int. Edn* **37**, 2202–2205 (1998).
24. Spector, M. S. & Zasadzinski, J. A. Topology of multivesicular liposomes, a model biliquid foam. *Langmuir* **12**, 4704–4708 (1996).
25. Klug, A. & Caspar, D. L. D. The structure of small viruses. *Adv. Vir. Res.* **7**, 225–325 (1960).
26. Crick, F. H. & Watson, J. D. The structure of small viruses. *Nature* **177**, 473–475 (1956).

Supplementary information is available from Nature's World-Wide Web site (<http://www.nature.com>) or as paper copy from the London editorial office of Nature.

**Acknowledgements**

We thank G. Sukhorukov and O. Tiourina for help in confocal optical microscopy, and

I. Erk for cryo-TEM. We also thank J.-L. Sikorav, P. Timmins and B. W. Ninham for critical reading of the manuscript and suggestions.

Correspondence and requests for materials should be addressed to M.D. (e-mail: [duboism@scm.saclay.cea.fr](mailto:duboism@scm.saclay.cea.fr)).

.....  
**Stability of atmospheric CO<sub>2</sub> levels across the Triassic/Jurassic boundary**

Lawrence H. Tanner\*, John F. Hubert†, Brian P. Coffey‡§ & Dennis P. McInerney||

\* Department of Geography and Geosciences, Bloomsburg University, Bloomsburg, Pennsylvania 17815, USA

† Department of Geosciences, University of Massachusetts, Amherst, Massachusetts 01003, USA

‡ Department of Geological Sciences, Virginia Polytechnic Institute and State University, Blacksburg, Virginia 24061, USA

|| Environmental Risk Management, Fleet National Bank of Connecticut, Hartford, Connecticut 06102, USA

.....  
 The Triassic/Jurassic boundary, 208 million years ago, is associated with widespread extinctions in both the marine and terrestrial biota. The cause of these extinctions has been widely attributed to the eruption of flood basalts of the Central Atlantic Magmatic Province<sup>1–4</sup>. This volcanic event is thought to have released significant amounts of CO<sub>2</sub> into the atmosphere, which could have led to catastrophic greenhouse warming<sup>5–7</sup>, but the evidence for CO<sub>2</sub>-induced extinction remains equivocal. Here we present the carbon isotope compositions of pedogenic calcite from palaeosol formations, spanning a 20-Myr period across the Triassic/Jurassic boundary. Using a standard diffusion model<sup>8,9</sup>, we interpret these isotopic data to represent a rise in atmospheric CO<sub>2</sub> concentrations of about 250 p.p.m. across the boundary, as compared with previous estimates of a 2,000–4,000 p.p.m. increase<sup>4,5</sup>. The relative stability of atmospheric CO<sub>2</sub> across this boundary suggests that environmental degradation and extinctions during the Early Jurassic were not caused by volcanic outgassing of CO<sub>2</sub>. Other volcanic effects—such as the release of atmospheric aerosols or tectonically driven sea-level change—may have been responsible for this event.

The mass extinction at the end of the Triassic claimed about 80% of all species<sup>10</sup>, including most non-dinosaurian archosaurs<sup>11</sup>. Although extinctions in the terrestrial and marine environments may be slightly asynchronous, they are closely related temporally and undoubtedly share causality<sup>12</sup>. This biotic crisis has been attributed previously to bolide impact<sup>6,13</sup> and sea-level change<sup>14,15</sup>. However, dating of the best-candidate impact structure (the Manicouagan crater) places the impact roughly 14 Myr earlier<sup>16</sup>, and sea-level change fails to explain the fern spike in the terrestrial boundary record<sup>6</sup>. The prevailing view is that this event resulted from the eruptions of the Central Atlantic Magmatic Province (CAMP), which may have produced as much as 7 × 10<sup>6</sup> km<sup>2</sup> of flood basalt in as little as 2 Myr<sup>3</sup>. CAMP volcanics include the basalts of the Newark Supergroup of eastern North America whose ages of around 200 Myr and stratigraphical proximity to the Triassic/Jurassic boundary are well constrained<sup>12,17</sup>. A frequently cited deleterious effect of these widespread, massive eruptions is a sudden increase in

§ Present address: ExxonMobil Upstream Research Company, Houston 77252, Texas, USA.

atmospheric CO<sub>2</sub> ( $p_{\text{CO}_2}$ ) from outgassing, resulting in intense global warming<sup>4–7</sup>.

The estimation of atmospheric palaeo- $p_{\text{CO}_2}$  using  $\delta^{13}\text{C}$  of pedogenic carbonate and the diffusion-reaction model is now common practice<sup>8,9,18</sup>. The carbon isotopic composition of soil carbonate is controlled by: the  $C_4/C_3$  vegetation ratio; the depth of carbonate accumulation; the temperature of carbonate precipitation; the isotopic composition of atmospheric carbon, a value well constrained by studies of marine carbonates; and soil productivity ( $S(z) = p_{\text{CO}_2,\text{soil}} - p_{\text{CO}_2,\text{atmos}}$ ), which is largely dependent on climatic regime. Values of palaeo- $p_{\text{CO}_2}$  derived from  $\delta^{13}\text{C}$  are similar to values from other sources, such as geochemical modelling<sup>19</sup>. Elevated palaeo- $p_{\text{CO}_2}$  for the Late Triassic has been estimated previously from the isotopic analysis of calcite in palaeosols<sup>8,9,18</sup>, but reliable data gathered with modern sampling protocols<sup>9,18</sup> are lacking for the Early Jurassic.

Our data were generated by sampling micritic calcite of pedogenic origin in mature, morphologically similar palaeosols in the rift basins of the Newark Supergroup of eastern North America and a continental basin of the southwestern United States (Fig. 1). The 21 samples comprise a data set that is tightly constrained by field and petrographical criteria to minimize variations in the composition of soil carbonate that result from differences in the depth of calcite accumulation and soil productivity. These samples represent discrete, mudstone-hosted, micritic nodules that occur in mature palaeosol profiles in which the upper part of the profile is characterized by a horizon of coalesced nodules (Bk) or laminar calcite (K). We selected samples from depths of 30 cm or greater, below the top of the Bk or K horizon, thereby minimizing the effects of soil depth<sup>9,18</sup>. Micritic calcite was selectively removed by microdrilling from thin section billets. The stratigraphic units sampled are: the Chatham Group (Carnian) of the Deep River basin, the New Haven Formation (Norian) of the Hartford basin, the McCoy Brook Formation (Hettangian) of the Fundy basin, and the Owl Rock Formation (Norian) of the Chinle group in the Chinle basin (Fig. 1).

These soils all formed on alluvial floodplains at low palaeolatitudes ( $\leq 15^\circ$ ) and most profiles show features such as gradational lower boundaries, rhizoliths, and circumgranular cracking, which suggest semi-arid to arid conditions, and so have been inferred to represent well-drained soils<sup>20–23</sup>.

The mean  $\delta^{13}\text{C}$  values for calcite in palaeosols from the Chatham Group, New Haven Formation, and Owl Rock Formation coincide within the limits of measurement, averaging  $-7.4\text{‰}$  relative to PeeDee Belemnite (PDB) (Table 1). Calcite from McCoy Brook Formation palaeosols is slightly heavier, with a mean  $\delta^{13}\text{C}$  of  $-7.1\text{‰}$  PDB (Table 1). This concordance suggests that these palaeosols formed under similar conditions of atmospheric composition and climate (warm, semi-arid to arid). The consistent isotopic compositions of pedogenic calcite is notable because these basins extend across about  $17^\circ$  of palaeolatitude, from the equatorial Deep River basin to the Fundy basin at about  $15^\circ\text{N}$  (ref. 24). Application of the diffusion-reaction model to these results requires several assumptions that (admittedly) introduce substantial room for variability in the calculated palaeo- $p_{\text{CO}_2}$ . The  $\delta^{13}\text{C}_{\text{atmos}}$  is set at  $-6.5\text{‰}$  PDB<sup>9</sup>, although variation in the composition of marine carbonates suggests that this value varied slightly during the early Mesozoic<sup>18</sup>. The  $\delta^{13}\text{C}$  value for organic matter was taken as  $-24\text{‰}$  PDB, consistent with direct measurements<sup>9</sup> and proxy measurements<sup>18</sup> for Upper Triassic and Lower Jurassic palaeosols. Fractionation of soil CO<sub>2</sub> by  $1\text{‰}$  relative to organic matter is assumed<sup>9</sup>. The temperature of carbonate precipitation within the soil is set at  $25^\circ\text{C}$  for these low-latitude palaeosols.

Potentially, the greatest source of variation in this calculation is the soil CO<sub>2</sub> productivity  $S(z)$ , controlled largely by precipitation and drainage characteristics of the soil. The morphologies of these palaeosols suggest formation in well-drained arid to semi-arid soils in which  $S(z)$  may vary from 3,000–7,000 p.p.m. (ref. 18). A mean  $S(z)$  value of 5,000 p.p.m. was chosen for these calculations. The combined mean  $\delta^{13}\text{C}$  of  $-7.4\text{‰}$  for Late Triassic pedogenic calcites (Chatham Group, New Haven Formation and Owl Rock Forma-

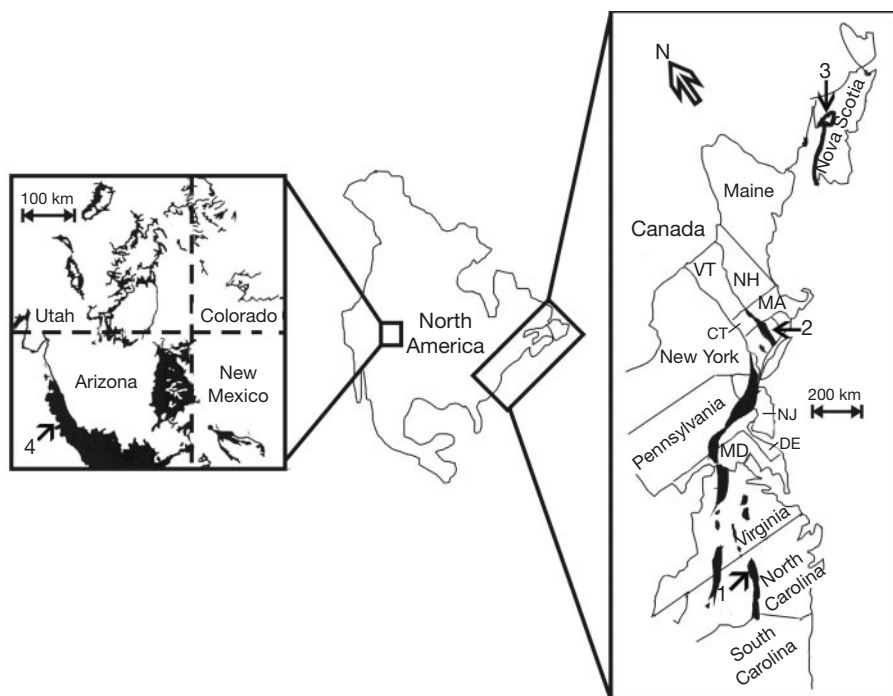


**Figure 1** Location of basins containing the sampled palaeosols. Right, exposed basins of the Newark Supergroup. Sampled basins: 1, Durham sub-basin of the Deep River basin (Chatham Group samples from the eastern Durham sub-basin); 2, Hartford basin (New

Haven Formation); and 3, Fundy basin (McCoy Brook Formation). Left, part of the Chinle basin with the outcrop pattern of the Chinle Group shown in black. Location of the sample area of the Owl Rock Formation is indicated (4).

**Table 1 Isotopic data**

	Sample	$\delta^{13}\text{C}_{\text{‰}}$ PDB
Upper Triassic palaeosols		
Chatham Group (Carnian)	94-7-1	-7.4
	94-7-2	-7.3
	94-7-2B	-7.4
	94-7-7	-7.4
	94-7-8	-7.3
New Haven Formation (Norian)	S-35	-7.5
	M17-S12	-7.3
Owl Rock Formation (Norian)	OR-1	-7.8
	EC-1	-7.6
	EC-1B	-6.8
	EC-2	-7.4
	EC-2B	-6.8
	EC-3	-7.3
	EC-3B	-7.6
	EC-4	-7.9
Mean	(n = 15)	-7.4 ( $\sigma = 0.3$ )
Lower Jurassic palaeosols		
McCoy Brook Formation (Hettangian)	MP1-1	-6.2
	MP1-2	-7.1
	MP1-2B	-7.0
	MP2-2	-7.6
	MP2-2B	-7.5
	MP2-3	-7.3
Mean	(n = 6)	-7.1 ( $\sigma = 0.5$ )

Analyses performed by Coastal Science Laboratories, Austin, Texas. Values are accurate to 0.2‰.

tion) yields a palaeo- $p_{\text{CO}_2}$  value of 2,250 p.p.m., about eight times the modern (pre-industrial) level, with a potential range of 1,350–3,150 p.p.m. (for  $S(z)$  values of 3,000 and 7,000). Calculation of palaeo- $p_{\text{CO}_2}$  using the McCoy Brook Formation data, yields slightly higher values of 2,480 p.p.m., within a possible range of 1,490–3,470 p.p.m.. Owing to the temperature control on isotope fractionation<sup>8</sup>, the difference between the Upper Triassic and Lower Jurassic palaeosols is eliminated if the mean temperature of pedogenic calcite precipitation were 2 °C lower in the more northerly Fundy basin. Our results are similar to previous estimates of palaeo- $p_{\text{CO}_2}$  for the Late Triassic<sup>8</sup> and the Late Jurassic<sup>25</sup>; however, these earlier estimates lacked the stratigraphical resolution necessary to examine changes in palaeo- $p_{\text{CO}_2}$  across the Triassic/Jurassic boundary. These estimates and ours are contained within the range of error for average palaeo- $p_{\text{CO}_2}$  for the latest Triassic and earliest Jurassic calculated by carbon-cycle modelling of 3–8 times the modern level<sup>19</sup>. Most significantly, our results differ substantially from previously published analyses for the McCoy Brook Formation (Lower Jurassic), which were obtained by bulk analyses of samples collected without the constraint of position within the palaeosol profile<sup>26</sup>.

The isotopic composition of oolitic goethite has been cited as evidence for greatly elevated (possibly 18 times the modern level)  $p_{\text{CO}_2}$  during the Early Jurassic<sup>4</sup>; however, the age of these data are not well constrained and are still subject to interpretation. Within the accuracy of measurement, our data do not indicate a significant increase in palaeo- $p_{\text{CO}_2}$  across the Triassic/Jurassic boundary. We do not therefore support an interpretation of sudden global warming resulting from CO<sub>2</sub> outgassing during CAMP volcanism. Suggestions of large increases in Early Jurassic palaeo- $p_{\text{CO}_2}$  due to CAMP eruptions seem to be made on the basis of gross overestimates of the CO<sub>2</sub> contribution from this magmatism. Recent estimates of the maximum volume of CAMP basalt<sup>3</sup> are comparable to the largest estimates for the Deccan Traps flood basalts<sup>27</sup>, the eruptions of which are estimated to have increased atmospheric CO<sub>2</sub> by only 200–250 p.p.m.v. (against a Late Cretaceous background of about 600 p.p.m.v.)<sup>28</sup>. This calculation, moreover, is based on an estimate of 0.5% CO<sub>2</sub> in the basaltic magma that may be overgenerous<sup>29</sup>. Therefore, we conclude that eruptions of the CAMP flood basalts were unlikely to have greatly increased palaeo- $p_{\text{CO}_2}$  during the Early Jurassic. Alternative mechanisms for extinction need to be explored more fully, particularly short-term

cooling or acidification of the atmosphere and oceans from SO<sub>2</sub> aerosols<sup>6,30</sup>, and rapid sea-level change driven by plume-driven thermal doming and collapse<sup>7</sup>. Although little evidence has been presented to support the former<sup>14</sup>, the latter hypothesis has the advantage of explaining the transgressive–regressive couplet that spans the Triassic/Jurassic boundary<sup>14,15</sup> and the widespread record of Early Jurassic marine anoxia<sup>14</sup>. □

Received 16 January; accepted 2 April 2001.

- Stothers, R. B. Flood basalts and extinction events. *Geophys. Res. Lett.* **20**, 1399–1402 (1993).
- Courtillot, V. Mass extinctions in the last 300 million years: one impact and seven flood basalts? *Israel J. Earth Sci.* **43**, 255–266 (1994).
- Marzoli, A. *et al.* Extensive 200-million-year-old continental flood basalts of the central Atlantic province. *Science* **284**, 616–618 (1999).
- Yapp, C. J. & Poths, H. Carbon isotopes in continental weathering environments and variations in ancient atmospheric CO<sub>2</sub> pressure. *Earth Planet. Sci. Lett.* **137**, 71–82 (1996).
- McElwain, J. C., Beerling, D. J. & Woodward, F. I. Fossil plants and global warming at the Triassic–Jurassic boundary. *Science* **285**, 1386–1390 (1999).
- Olsen, P. E. Giant lava flows, mass extinctions, and mantle plumes. *Science* **284**, 604–605 (1999).
- Hallam, A. The end-Triassic extinction in relation to a superplume event. *Geol. Soc. Am. Abs. Prog.* **37**, 380 (2000).
- Cerling, T. E. Carbon dioxide in the atmosphere: evidence from Cenozoic and Mesozoic paleosols. *Am. J. Sci.* **291**, 377–400 (1991).
- Cerling, T. E. Stable carbon isotopes in paleosol carbonates. *Spec. Publ. Int. Ass. Sediment.* **27**, 43–60 (1999).
- Sepkoski, J. J. Jr. in *Global Events and Event Stratigraphy in the Phanerozoic* (ed. Walliser, O. H.) 35–51 (Springer, Berlin, 1996).
- Curtis, K. & Padian, K. An Early Jurassic microvertebrate fauna from the Kayenta Formation of northeastern Arizona; microfaunal change across the Triassic–Jurassic boundary. *PaleoBios* **19**, 19–37 (1999).
- Pálffy *et al.* Timing the end-Triassic mass extinction: first on land, then in the sea? *Geology* **28**, 39–42 (2000).
- Olsen, P. E., Shubin, N. H. & Anders, M. H. New Early Jurassic tetrapod assemblages constrain Triassic–Jurassic tetrapod extinction event. *Science* **237**, 1025–1029 (1987).
- Hallam, A. & Wignall, P. B. *Mass Extinctions and Their Aftermath* (Oxford, New York, 1997).
- Hallam, A. & Wignall, P. B. Mass extinctions and sea-level changes. *Earth Sci. Rev.* **48**, 217–250 (1999).
- Hodych, J. P. & Dunning, G. R. Did the Manicouagan impact trigger end-of-Triassic mass extinction? *Geology* **20**, 51–54 (1992).
- Fowell, S. J. & Olsen, P. E. Time calibration of Triassic/Jurassic microfossil turnover, eastern North America. *Tectonophysics* **222**, 361–369 (1993).
- Ekart, D. D., Cerling, T. E., Montañez, I. P. & Tabor, N. J. A 400 million year carbon isotope record of pedogenic carbonate: implications for paleoatmospheric carbon dioxide. *Am. J. Sci.* **299**, 805–827 (1999).
- Berner, R. A. Enriched: GEOCARB II; a revised model of atmospheric CO<sub>2</sub> over Phanerozoic time. *Am. J. Sci.* **294**, 56–91 (1994).
- Hubert, J. F. Paleosol caliche in the New Haven Arkose, Newark Group, Connecticut. *Palaeogeogr. Palaeoclimatol. Palaeoecol.* **24**, 151–168 (1978).
- Coffey, B. P. & Textoris, D. A. Paleosols and paleoclimatic evolution, Durham sub-basin, North Carolina. *Geol. Nat. Hist. Sur. Connecticut Misc. Rep.* **1**, 6 (1996).
- Tanner, L. H. in *The Continental Jurassic* (ed. Morales, M.) 656–574 (Museum of Northern Arizona, Flagstaff, Arizona, 1996).
- Tanner, L. H. Palustrine-lacustrine and alluvial facies of the (Norian) Owl Rock Formation (Chinle Group), Four Corners region, southwestern U.S.A.: implications for Late Triassic paleoclimate. *J. Sedim. Res.* **70**, 1280–1289 (2000).
- Olsen, P. E. Stratigraphic record of the early Mesozoic breakup of Pangea in the Laurasia-Gondwana rift system. *Annu. Rev. Earth Planet. Sci.* **25**, 337–401 (1997).
- Ekart, D. D. & Cerling, T. E. PCO<sub>2</sub> during deposition of the Late Jurassic Morrison Formation and other paleoclimatic/ecologic data as inferred by stable carbon isotope analyses. *Geol. Soc. Am. Abs. Prog.* **28**, 252 (1996).
- Suchecki, R. K., Hubert, J. F. & De Wet, C. B. Isotopic imprint of climate and hydrogeochemistry on terrestrial strata of the Triassic–Jurassic Hartford and Fundy rift basins. *J. Sed. Res.* **58**, 801–811 (1988).
- Coffin, M. F. & Eldholm, O. Scratching the surface: estimating dimensions of large igneous provinces. *Geology* **21**, 515–518 (1993).
- Caldeira, K. G. & Rampino, M. R. Deccan volcanism, greenhouse warming, and the Cretaceous/Tertiary boundary. *Geol. Soc. Am. Spec. Pap.* **247**, 117–123 (1990).
- Wallace, P. & Anderson, A. T. in *Encyclopedia of Volcanoes* (ed. Sigurdsson, H.) 149–170 (Academic, New York, 2000).
- Parfitt, E. A. & Wilson, L. Impact of basaltic eruptions on climate. *Geol. Soc. Am. Abs. Prog.* **32**, 501 (2000).

**Acknowledgements**

This study was supported by grants from the Research and Disciplinary Fund and the Special Initiative Fund, Bloomsburg University (L.H.T.), and from the Connecticut Department of Environmental Protection (D.P.I.). We thank the Navajo nation for permitting us to conduct research on reservation lands. We also thank S. Driese, D. Fastovsky and A. Hallam for their comments on this manuscript.

Correspondence and requests for materials should be addressed to L.H.T. (e-mail: lhtann@sunlink.net).

Reproduced with permission of the copyright owner. Further reproduction prohibited without permission.